THE LANCET
Public Health

Supplementary appendix

This appendix formed part of the original submission and has been peer reviewed. We post it as supplied by the authors.

Supplement to: García-León D, Masselot P, Mistry MN, et al. Temperature-related mortality burden and projected change in 1368 European regions: a modelling study. *Lancet Public Health* 2024; published online Aug 21. https://doi.org/10.1016/S2468-2667(24)00179-8.

Supplementary Material

Temperature-related mortality burden and projected change in 1368 European regions: a modelling study

David García-León PhD*, Pierre Masselot PhD, Malcolm N Mistry PhD, Prof Antonio Gasparrini PhD, Corrado Motta MSc, Luc Feyen PhD, and Juan-Carlos Ciscar PhD.

*Corresponding author: David García-León, email: david.garcia-leon@ec.europa.eu. European Commission, Joint Research Centre, Edificio Expo, Inca Garcilaso 3, 41092 Seville, Spain.

A. Exposure Response Functions' modelling details

Exposure-response functions (ERFs) were originally estimated for a subsample of 232 cities for which daily time series of mortality were available through the MCC dataset, then extrapolated to the whole sample of 854 cities.[1] The modelling process followed three main stages: i) city and age-group specific overall cumulative exposure-response functions were estimated in 232 MCC cities, ii) these ERFs were then pooled into a predictive meta-regression model using age and composite indices of vulnerability as predictors, and iii) ERFs were predicted in the 854 cities from the meta-regression model, combined with a Kriging approach to model uncaptured spatial patterns.

In the first stage, we estimated age group-specific ERF through a quasi-Poisson time series model for each of the 232 MCC cities (https://mccstudy.lshtm.ac.uk/). We applied a distributed lag nonlinear model (DLNM)[2] with standard parameterization.[3] In the temperature dimension, we specified a quadratic B-spline with knots positioned at the 10th, 75th and 90th percentile of the city-specific temperature distribution, and in the lag dimension a cubic natural spline with three knots positioned at equally-spaced log-values using a lag period of 21 days. We also included indicators for the day of the week and a natural spline of time with seven degrees of freedom per year to control for time-varying confounding. Once the model was fit, we extracted the coefficients $\widehat{\boldsymbol{\theta}}_{ij}$ representing the overall cumulative exposure response function for age group j of city *i*.[4]

In the second stage, we pooled the age- and city-specific reduced first stage coefficients in a meta-regression model[5] as follows:

$$\widehat{\boldsymbol{\theta}}_{\boldsymbol{ij}} = \boldsymbol{\gamma}_{r(i)} + ns(a_{ij}) + \boldsymbol{X}_i\boldsymbol{\beta} + \boldsymbol{b}_i + \boldsymbol{\varepsilon}_{ij} \quad (1)$$

where $\boldsymbol{\gamma}_{r(i)}$ is a term representing the region of city i, $ns(a_{ij})$ is a natural spline of the age a_{ij} associated to $\widehat{\boldsymbol{\theta}}_{ij}$, $\boldsymbol{X}_i$ is a set of five city-specific composite indices of vulnerability with $\boldsymbol{\beta}$ the associated coefficients, $\boldsymbol{b}_i$ is a city-specific random effect and $\boldsymbol{\varepsilon}_{ij}$ is the residual of the model. The term $r(i)$ represents four cardinal regions in Europe, as defined by the M49 UN classification.[6] Age a_{ij} was computed as the average age of death within each available age-group within the MCC dataset, estimated through age-specific baseline death rates. Composite indices of vulnerability were computed by principal component analysis (PCA) on 22 socio-economic, environmental and topological city characteristics, detailed elsewhere.[1] We extracted the first five principal components. All modelling choices, i.e. the number of components, age term and regional background specification were selected by minimising the AIC across many varied specifications.

From the model (1), we extracted the best linear unbiased predictor (BLUP) residuals[7,8] as estimates of $\boldsymbol{b}_i$ and performed a Kriging on these residuals. These allowed us to obtain an estimate of the random effect $\boldsymbol{b}_i$ in all locations not featured in the first stage, and include smooth spatial patterns not captured by the fixed effects of model (1). The final ERF in each location and for each age group was the sum of predictions from model (1), and extrapolation from the Kriging on BLUP residuals.

B. Modelling differential risks by age

The first-stage time series regression model was performed on each age group in the MCC dataset, with age groups differing by country. However, the number of deaths recorded can be very low for the youngest age groups in smaller cities, resulting in unstable first-stage estimates and low statistical power.[9] Therefore, when the total death count in the series is below 5,000 for an age group, we aggregated it with the older one when available. Because the age groups differ between countries in the MCC dataset, we included age as a continuous age variable $a_{ij} \in [0; 100]$ in the second-stage model. For each city i and each age group j available in the first stage, we computed an associated average age of death a_{ij} as a simple weighted mean of the ages within the group, i.e.:

$$a_{ij} = \frac{\sum_{k=l}^{u} w_{ik} k}{\sum_{k=l}^{u} w_{ik}} \quad (2)$$

where l and u are the age boundaries of the group and wik are the death rates associated with age k in city i. Note that for the oldest age group, we instead used the life expectancy at the lower bound (e.g. at 85 for the group 85 and older). Death rates and life expectancy are extracted for each city from Eurostat. The average ages of death a_{ij} were then included as a continuous linear term in the second stage model. Nonlinear terms of age through a natural spline with various knot placements were also investigated but resulted in highest AIC compared to the linear term. For predictions at age groups in the third stage, we repeated the process. For each city and each age group considered, we computed the average age of death within this age group using equation (2), or alternatively we used life expectancy at 85 for age group 85 and older.

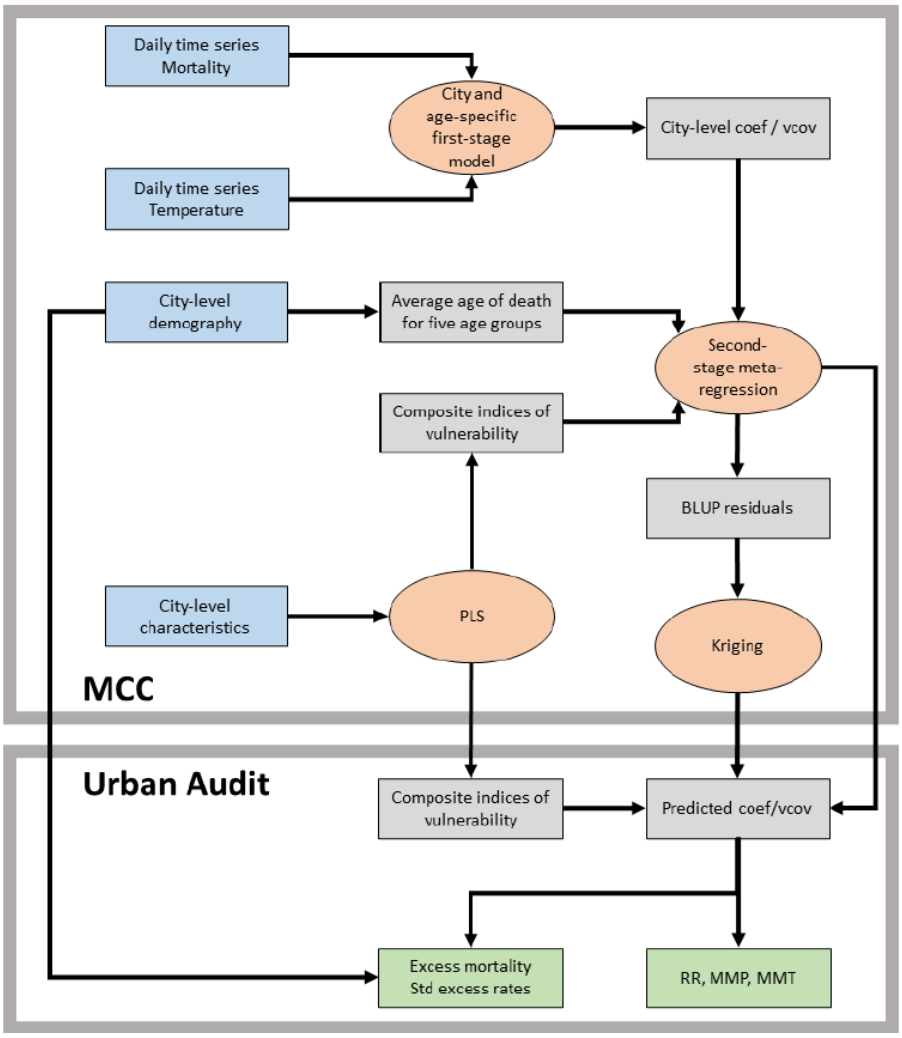

Figure S1: Flowchart describing the modelling framework. Squares represent input/output data while ellipses represent models/processes. Blue represents input data, grey derived data and green output data.

It should be noted that, from a methodological point of view, it could have been feasible to model risk continuously also across the age spectrum. This was the modelling strategy adopted in Masselot et al. (2023).[1] However, the present exercise adds extra layers of complexity, as 22 climate models had to be processed and projections over a time span of 120 years had to be produced. To reduce the dimensionality of the problem and for the sake of computational efficiency, we decided to adhere to representative age groups, as indicated in the main text. Even in this reduced setup, we handled approximately 6.65 billion cases (1,368 Regions x 365 days x 121 years x 11 climate models x 2 emission scenarios x 5 age groups).

C. Global Warming Level analysis: a time sampling approach

We adopt the time sampling approach to select climate conditions at different Global Warming Levels (GWLs) under the two transient pathways considered, an approach also employed in IPCC's AR6[10] (see Cross-Chapter Box 11.1, Figure 3; https://www.ipcc.ch/report/ar6/wg1/figures/chapter-11/ccbox-11-1-figure-3). The time sampling approach assumes that the climate stressor at a certain GWL can be derived from the transient climate projections by considering climate over a 30-year time window centred on the year when the targeted GWL is reached. This method allows us to separate climate from the time at which a specific GWL is reached, enabling us to assess how climate stressors under different GWLs affect future societies (in this case, at the end of the century).

In Hsiang et al. (2017, Figure 5),[11] it is demonstrated that for a range of climate impacts at different global warming levels, the within Representative Concentration Pathway (RCP) variability is comparable to the between RCP variability. Other studies also indicate that for most variables and hazards (e.g. river floods, droughts), the effect of the pathway to reach a GWL over Europe is small compared to the climate model variability, and the projections of the two pathways for the GWLs can be merged into a single ensemble without significant loss of information.[12,13] These and other recent studies (also included in AR6) using the time sampling approach demonstrate that for a given GWL, the variability in regional temperature projections between climate models forced by the same RCP is of the same order as the variability between models forced by different RCPs.

Table S1 (appendix p 5) details the year when the specific warming levels are reached for each combination of RCM-GCM and the two RCPs considered.

D. Regional aggregation and extrapolation: further considerations and some examples

In cases where no city information is available for a specific NUTS 3 region, we use the 'm' cities available in the NUTS 2 to which that NUTS 3 belongs (NUTS 3 $\subset$ NUTS 2) to calculate a composite city in the same fashion as described before. We then use that composite city for extrapolation to the population of the NUTS 3 without city data based on the fraction of each population group of the analysed NUTS 3 within its higher-level NUTS 2. We applied the same rationale to construct NUTS 1 or NUTS 0 composite cities, where applicable. Standardised death rates were obtained by dividing the total attributable number of deaths in each NUTS 3 region by 100,000.

Below are some real examples of how the extrapolation methodology is applied:

- Multiple cities sampled in a NUTS 3 region. For the NUTS 3 region ES618 (Seville, Spain) mortality data for three cities are available: Seville (City), Dos Hermanas and Alcalá de Guadaira. We construct a composite cite out of these three cities and obtain the attributable number of deaths in that composite city for cold and heat and the different age groups. Attributable deaths in region ES618 would be those of the composite city rescaled by the fraction of each population group of the composite city in the total age group population of region ES618.
- No city data available in a specific NUTS 3 and other cities sampled in NUTS 2 (NUTS 3 $\subset$ NUTS 2). Attributable deaths in ES416 (Segovia, Spain) will emerge after rescaling deaths of a composite city built for ES41 (Castilla y León, Spain), based on the eight available cities in ES41.
- No city data available in a specific NUTS 3 and only one city sampled in NUTS 2 (NUTS 3 $\subset$ NUTS 2). Attributable deaths in ES241 (Huesca, Spain) would be those of Zaragoza (ES243), the only city sampled in NUTS 2 region of Aragón (ES24), conveniently rescaled by population weights.

In selecting the method of aggregation, our aim was to confer a structure to regions lying within the same NUTS unit (the political entity of reference). However, we certainly did not overlook the sensitivity of our results to different aggregation methods. An alternative would have been to just look at neighbouring regions, irrespective of whether they belong to the same higher-order NUTS unit or not. We felt that this was not a good idea, as the NUTS classification plays a specific role in shaping a number of EU policies. For example, regions eligible for support from cohesion policy have been defined at the NUTS 2 level (https://ec.europa.eu/eurostat/web/nuts/overview).

Nevertheless, we provide comparisons of our estimates with other studies covering Europe and more local areas, and our numbers largely align with most of them, suggesting that our aggregation and extrapolation methods are sound.

E. Comparison of our estimates with findings from existing literature

The figures shown in this article are comparable to recent estimates in the literature but also reveal discrepancies with others, underscoring the complexities inherent in modelling and projecting climate-related health impacts. Ballester et al. (2023)[14] reported that in 2022, there were 61,672 deaths (95% eCI: 37–86 thousand) attributed to heat in 35 European countries, including the 30 countries analysed here (representing 98.1% of the total population analysed). This contrasts with our baseline value of 43,700. However, climate conditions in the last few years, particularly in the very warm years 2022 and 2023, may well resemble a +1·5°C climate.[15,16] In this case, the number of heat-related deaths projected by our analysis for +1·5°C, after adjusting our estimates for the contribution of population and total death rate dynamics, amounts to 60,944 (95% eCI: 50·1–72·6 thousand). This aligns more closely with the findings of these authors. On a more local level, our projections of heat-related mortality for the UK align very closely with Jenkins et al. (2022)[17] for both current and future warming scenarios. Huber et al. (2020)[18] predict that the ratio of cold to heat deaths in Germany will drop from 5·9:1 today to 1·6:1 under +3°C, which compares well to our projections (5·3:1 today versus 1·9:1 under +3°C). Vicedo-Cabrera et al. (2023)[19] estimate 623 deaths attributed to heat in Switzerland in 2022, which compares to our baseline value of 583 (95% eCI: 458–668). For the same country, de Schrijver et al. (2023)[20] estimate a cold death rate of 49 deaths per 100,000 people over the period 2009-2017, aligning with our estimated value (47·2). However, their estimated heat death rate (2·1) differs from ours (8·3). This discrepancy might be influenced by their sample period, which does not cover long and intense episodes of heatwaves affecting their territory.[21] The estimates reported by Tobías et al. (2023)[22] for the case of Spain (11,100 in 2023) do not compare well to our estimates under +1·5°C (adjusted by population dynamics) of 7,576 deaths (95% eCI: 6·9–9·0 thousand) but resemble those under +2°C warming of 10,741 (95% eCI: 9·7–13·0 thousand). This indicates that in recent years, southern Europe might be experiencing harsher summers than the rest of Europe.[23] Finally, in Masselot et al. (2023),[1] (the study we expand on), the reported mortality estimates represent around 40% of the EU population.26 Their current annual total of 150,000 deaths—135,000 due to cold and 15,000 due to heat (a ratio of 9:1)—should be rescaled by a factor of 2·5 to match the total population, implicitly assuming equal vulnerability between regional population and those living in urban environments. This yields 375,000 deaths (337,500 + 37,500), which aligns with the figures reported here and validates our aggregation and extrapolation approach.

F. Supplementary Tables and Figures

Table S1: Climate models (RCM-GCM) considered in the analysis and the years at which global warming levels are reached under emission scenarios RCP4·5 and RCP8·5.

RCM	GCM	+1·5°C		+2°C		+3°C		+4°C	
		RCP4·5	RCP8·5	RCP4·5	RCP8·5	RCP4·5	RCP8·5	RCP4·5	RCP8·5
CLMcom-CCLM4-8-17	CNRM-CERFACS-CNRM-CM5	2035	2029	2057	2044		2067		2089
CLMcom-CCLM4-8-17	ICHEC-EC-EARTH	2033	2026	2056	2041		2066		2090
CLMcom-CCLM4-8-17	MPI-M-MPI-ESM-LR	2034	2028	2064	2044		2067		2089
DMI-HIRHAM5	ICHEC-EC-EARTH	2032	2028	2054	2043		2065		2086
IPSL-INERIS-WRF331F	IPSL-IPSL-CM5A-MR	2023	2021	2042	2035		2054		2073
KNMI-RACMO22E	ICHEC-EC-EARTH	2032	2026	2056	2042		2065		2087
SMHI-RCA4	CNRM-CERFACS-CNRM-CM5	2035	2029	2057	2044		2067		2089
SMHI-RCA4	ICHEC-EC-EARTH	2033	2026	2056	2041		2066		2090
SMHI-RCA4	IPSL-IPSL-CM5A-MR	2023	2021	2042	2035		2054		2073
SMHI-RCA4	MOHC-HadGEM2-ES	2021	2018	2037	2030	2069	2051		2071
SMHI-RCA4	MPI-M-MPI-ESM-LR	2034	2028	2064	2044		2067		2089

For +4°C, models extrapolated based on Ballari et al. (2018)[24]. Only one common GCM (IPSL).

For models that show warming +4°C later than 2085, we take the period 2071-2100 to compute the stabilised climate time series

Table S2: NUTS and city metadata by country*.

	Country	Country Code	NUTS 3	NUTS 2	NUTS 1	No. cities analysed	Cities in MCC
1	Austria	AT	35	9	3	6	0
2	Belgium	BE	44	11	3	15	0
3	Bulgaria	BG	28	6	2	18	0
4	Croatia	HR	21	4	1	7	0
5	Cyprus	CY	1	1	1	3	3
6	Czechia	CZ	14	8	1	18	3
7	Denmark	DK	11	5	1	4	0
8	Estonia	EE	5	1	1	3	3
9	Finland	FI	19	5	2	9	1
10	France	FR	96	22	13	72	18
11	Germany	DE	401	38	16	127	12
12	Greece	EL	52	13	4	14	1
13	Hungary	HU	20	8	3	19	0
14	Ireland	IE	8	3	1	5	1
15	Italy	IT	107	21	5	87	16
16	Latvia	LV	6	1	1	10	0
17	Lithuania	LT	10	2	1	6	0
18	Luxembourg	LU	1	1	1	1	0
19	Malta	MT	2	1	1	1	0
20	Netherlands	NL	40	12	4	47	5
21	Norway	NO	11	6	1	4	1
22	Poland	PL	73	17	7	68	0
23	Portugal	PT	23	5	1	14	2
24	Romania	RO	42	8	4	35	8
25	Slovakia	SK	12	2	1	8	0
26	Slovenia	SI	8	4	1	2	0
27	Spain	ES	52	18	7	90	44
28	Sweden	SE	21	8	3	14	3
29	Switzerland	CH	26	7	1	12	8
30	United Kingdom	UK	179	41	12	135	103
31	European Union (EU-27)	EU	1,152	234	89	703	120
32	Europe (30 countries)	E3	1,368	288	103	854	232

*Overseas territories (NUTS1: FRY - Départements d'Outre Mer; NUTS2: ES70 – Canary Islands; NUTS3: PT200 - Região Autónoma dos Açores, PT300 - Região Autónoma da Madeira, NO0B1 - Jan Mayen, NO0B2 - Svalbard) were excluded from the analysis. MCC stands for the Multi-Country Multi-City Collaborative Research Network (https://mccstudy.lshtm.ac.uk/), an international collaboration of research teams working on a program aimed at producing epidemiological evidence on associations between environmental stressors, climate, and health.

Table S3: Projected median ratios of cold-related to heat-related deaths in Europe under present climate conditions (period 1991–2020, approximately equivalent to +1°C) and under four different warming scenarios. Median deaths were obtained as the 50th percentile of the death distributions originated by from the 11 climate models and two emission scenarios considered. Lower (Upper) values denote the 5th (95th) percentile of the death distribution. We used the current population (year 2020) for today's results and sociodemographic estimates for year 2100 for the respective warming scenarios**.**

	Ratio of Cold-Heat deaths				
	TODAY	**+1·5°C**	**+2°C**	**+3°C**	**+4°C**
Austria	5·9 (5·4-7·3)	4·6 (3·8-7·4)	3·5 (2·5-4·7)	2·0 (1·8-2·7)	1·1 (1·0-1·4)
Belgium	7·2 (6·5-8·2)	6·8 (5·3-9·3)	4·9 (3·9-7·6)	2·6 (2·2-4·4)	1·5 (1·2-2·4)
Bulgaria	9·7 (9·1-10·5)	6·6 (5·9-8·4)	5·0 (4·2-5·6)	2·9 (2·3-3·2)	1·6 (1·4-1·6)
Croatia	3·7 (3·6-3·9)	2·9 (2·6-3·2)	2·2 (1·9-2·6)	1·4 (1·3-1·5)	0·9 (0·8-0·9)
Cyprus	6·4 (6·0-6·8)	4·5 (4·2-4·9)	3·2 (3·0-3·6)	1·6 (1·5-1·8)	0·9 (0·8-1·0)
Czechia	12·9 (11·7-15·2)	9·6 (7·4-14·5)	7·2 (5·2-10·8)	4·1 (3·4-5·9)	2·4 (2·1-3·3)
Denmark	32·2 (27·4-35·6)	19·0 (12·3-29·4)	14·0 (8·9-22·0)	7·3 (4·3-10·2)	3·7 (2·1-5·7)
Estonia	25·5 (23·8-28·0)	16·9 (11·5-20·8)	13·1 (8·4-16·2)	8·1 (4·6-10·2)	4·7 (2·6-6·2)
Finland	34·0 (27·9-37·8)	20·5 (13·1-25·4)	15·1 (11·0-19·3)	8·4 (6·4-10·3)	4·7 (3·4-6·5)
France	10·2 (9·1-11·8)	7·9 (6·7-9·9)	5·5 (4·3-7·9)	2·7 (2·2-3·7)	1·4 (1·2-2·1)
Germany	5·3 (4·9-6·0)	4·8 (3·5-6·7)	3·5 (2·8-5·3)	1·9 (1·7-2·9)	1·1 (1·0-1·7)
Greece	5·4 (5·1-5·6)	3·8 (3·5-4·3)	2·7 (2·5-2·9)	1·5 (1·3-1·6)	0·7 (0·7-0·8)
Hungary	10·2 (9·5-11·7)	7·7 (6·6-10·0)	6·5 (4·8-8·2)	3·9 (3·9-4·6)	2·4 (2·2-2·6)
Ireland	132·5 (95·2-188·6)	67·4 (52·4-107·7)	41·2 (30·7-69·1)	13·7 (11·6-27·9)	7·4 (5·4-13·8)
Italy	4·0 (3·9-4·3)	2·9 (2·5-3·2)	2·1 (1·8-2·6)	1·2 (1·0-1·4)	0·6 (0·6-0·8)
Latvia	14·8 (13·9-15·1)	11·8 (9·2-13·5)	9·7 (8·0-11·1)	7·0 (5·8-7·1)	4·7 (3·8-5·0)
Lithuania	15·0 (14·2-15·5)	11·7 (9·3-14·7)	10·0 (8·1-11·3)	7·1 (5·9-7·7)	4·8 (4·0-5·0)
Luxembourg	5·5 (5·0-6·9)	5·4 (4·1-8·2)	3·8 (2·9-5·6)	2·0 (1·6-3·0)	1·0 (0·9-1·6)
Malta	4·0 (3·9-4·3)	2·5 (2·0-3·0)	1·7 (1·4-2·1)	0·9 (0·6-1·0)	0·4 (0·3-0·5)
Netherlands	5·2 (4·9-5·7)	6·5 (4·8-8·5)	4·6 (3·7-6·8)	2·3 (2·1-3·9)	1·2 (1·2-2·1)
Norway	43·8 (34·7-54·5)	27·3 (17·4-41·1)	21·6 (11·7-34·0)	9·6 (6·0-13·5)	5·3 (3·1-7·2)
Poland	10·9 (10·3-12·4)	9·1 (6·9-11·7)	7·1 (5·3-9·5)	4·4 (3·9-5·6)	2·8 (2·4-3·4)
Portugal	7·3 (7·0-8·6)	5·8 (4·8-6·6)	4·1 (3·6-5·1)	2·0 (2·0-2·2)	1·1 (0·9-1·2)
Romania	10·1 (9·5-11·0)	7·4 (6·3-9·1)	5·6 (4·6-6·8)	3·6 (3·3-3·8)	2·1 (2·0-2·2)
Slovakia	9·9 (9·0-11·4)	7·5 (6·1-9·8)	6·1 (4·3-7·6)	3·5 (3·3-4·3)	2·1 (2·0-2·4)
Slovenia	3·3 (3·2-3·5)	2·7 (2·3-3·2)	2·1 (1·7-2·6)	1·3 (1·2-1·6)	0·8 (0·7-0·9)
Spain	5·1 (5·0-5·4)	3·8 (3·3-4·2)	2·5 (2·2-2·7)	1·2 (1·0-1·2)	0·5 (0·5-0·7)
Sweden	32·5 (27·5-36·3)	18·7 (12·8-29·2)	13·8 (9·7-22·3)	7·9 (4·5-9·6)	3·8 (2·7-5·5)
Switzerland	5·2 (4·6-6·6)	4·4 (3·4-6·8)	3·2 (2·4-4·5)	1·6 (1·3-2·1)	0·8 (0·7-1·2)
United Kingdom	51·0 (40·0-58·4)	31·8 (23·7-44·0)	21·4 (16·7-37·1)	8·2 (7·9-15·0)	4·9 (3·7-6·8)
EU-27	7·0 (6·7-7·6)	5·6 (4·7-6·7)	4·1 (3·4-5·0)	2·2 (1·9-2·7)	1·2 (1·1-1·5)
Europe	8·3 (8·0-9·1)	6·7 (5·6-8·1)	4·9 (4·0-6·1)	2·6 (2·3-3·3)	1·4 (1·3-1·8)

Table S4: Contribution of climate warming and demographic changes (lower fertility and declining death rates) to the projected variations in temperature-related mortality risk. Contributions were obtained as the difference between the time series simulations subject to demographic changes and under the absence of them**.**

	COLD			HEAT		
	Climate	Demography	Total	Climate	Demography	Total
Austria	-10·0	+15·3	+5·3	+16·0	+1·0	+17·0
Belgium	-10·8	+14·3	+3·5	+10·6	+0·0	+10·6
Bulgaria	-18·6	-20·6	-39·2	+26·6	-3·4	+23·2
Croatia	-18·7	-1·8	-20·5	+32·6	-3·1	+29·5
Cyprus	-21·4	+25·3	+4·0	+25·9	+2·6	+28·5
Czechia	-14·8	+7·4	-7·4	+12·1	+0·1	+12·1
Denmark	-18·4	+15·6	-2·8	+8·8	+0·7	+9·5
Estonia	-18·1	+8·5	-9·7	+8·6	+0·3	+8·9
Finland	-19·5	+35·8	+16·3	+8·8	+1·2	+10·0
France	-13·1	+19·9	+6·8	+14·7	+0·8	+15·5
Germany	-9·5	+3·7	-5·8	+12·5	-1·3	+11·2
Greece	-24·6	+20·9	-3·7	+41·1	+1·5	+42·6
Hungary	-16·7	-1·4	-18·1	+14·8	-1·2	+13·5
Ireland	-24·8	+64·2	+39·5	+6·6	+0·7	+7·4
Italy	-18·4	+13·7	-4·6	+36·0	+1·3	+37·4
Latvia	-17·6	-18·2	-35·8	+8·4	-1·7	+6·8
Lithuania	-16·7	-13·0	-29·7	+8·1	-1·1	+7·0
Luxembourg	-9·4	+25·3	+15·9	+16·1	+1·5	+17·6
Malta	-26·4	+41·1	+14·7	+72·9	+7·6	+80·4
Netherlands	-10·8	+16·2	+5·4	+9·1	-0·6	+8·6
Norway	-15·6	+33·1	+17·5	+7·8	+0·9	+8·7
Poland	-18·2	+28·2	+10·0	+12·7	+1·5	+14·2
Portugal	-23·9	+11·7	-12·3	+18·4	-0·1	+18·3
Romania	-19·7	+6·7	-13·0	+22·0	-0·3	+21·7
Slovakia	-20·2	+39·2	+19·0	+17·8	+2·8	+20·6
Slovenia	-12·2	+13·2	+1·0	+23·2	+1·0	+24·2
Spain	-17·6	+21·0	+3·4	+34·2	+1·5	+35·7
Sweden	-16·2	+18·0	+1·8	+7·8	+0·7	+8·6
Switzerland	-8·7	+13·5	+4·8	+18·4	+0·2	+18·6
United Kingdom	-18·9	+16·0	-2·8	+7·6	+0·5	+8·1
EU-27	-15·1	+12·0	-3·1	+19·2	-0·1	+19·2
Europe	-15·5	+13·1	-2·4	+17·4	-0·1	+17·3

Table S5: Projected total net effect on temperature-related mortality (the variation in heat-related deaths and cold-related deaths) for different age groups and the total population. Total aggregates may slightly differ from the sum of age group results, as values have been rounded to the nearest decimal.

COLD

Age	+1.5°C-Today	+2.0°C-Today	+3.0°C-Today	+4.0°C-Today
20-44	-2727	-2772	-2825	-3047
45-64	-25680	-25918	-26028	-27674
65-74	-41695	-42144	-42441	-45257
75-84	-59036	-60911	-63754	-70581
85+	+155826	+140400	+108228	+79747
TOTAL	+26688	+8655	-26820	-66813

HEAT

Age	+1.5°C-Today	+2.0°C-Today	+3.0°C-Today	+4.0°C-Today
20-44	-738	-649	-406	-75
45-64	-4282	-3901	-2806	-1321
65-74	-4810	-4218	-2513	-62
75-84	-5022	-3014	+2620	+11489
85+	+30014	+44723	+84898	+152854
TOTAL	+15162	+32941	+81794	+162885

COLD + HEAT

Age	+1.5°C-Today	+2.0°C-Today	+3.0°C-Today	+4.0°C-Today
20-44	-3465	-3421	-3231	-3122
45-64	-29962	-29819	-28834	-28995
65-74	-46506	-46362	-44954	-45318
75-84	-64058	-63925	-61134	-59093
85+	+185840	+185123	+193126	+232600
TOTAL	+41850	+41596	+54974	+96072

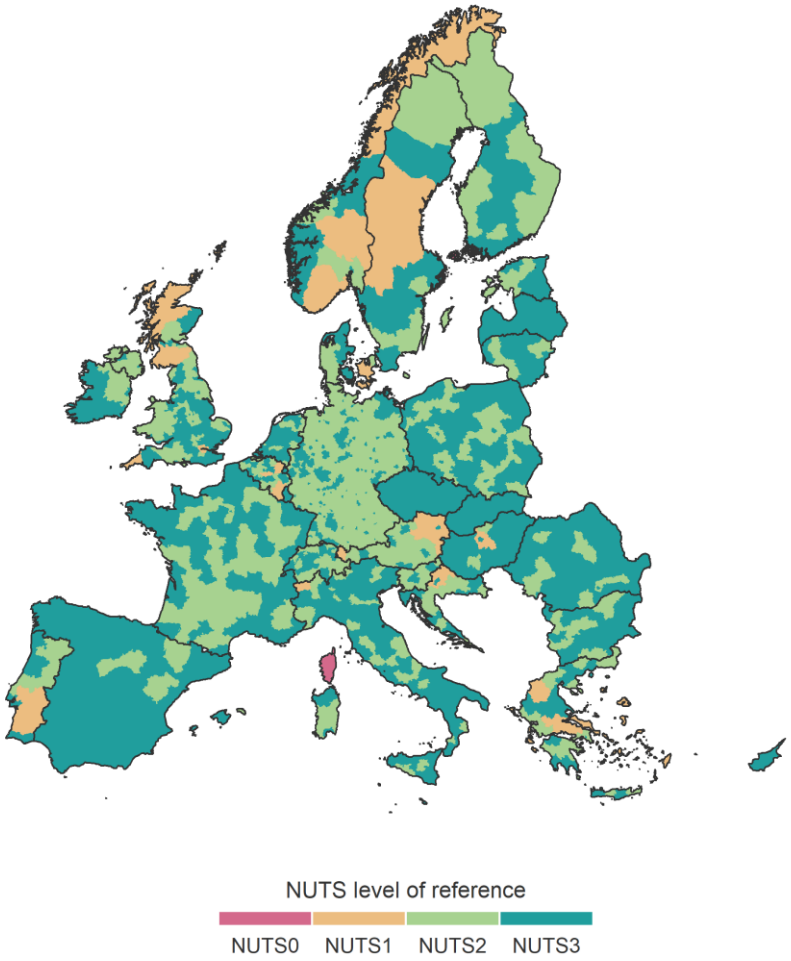

Figure S2: Map illustrating whether the regional NUTS 3 outcomes originate from the cities within the respective NUTS 3 regions or are derived by extrapolating values from the higher-level NUTS regions (NUTS 2, NUTS 1, or NUTS 0) to which they are affiliated.

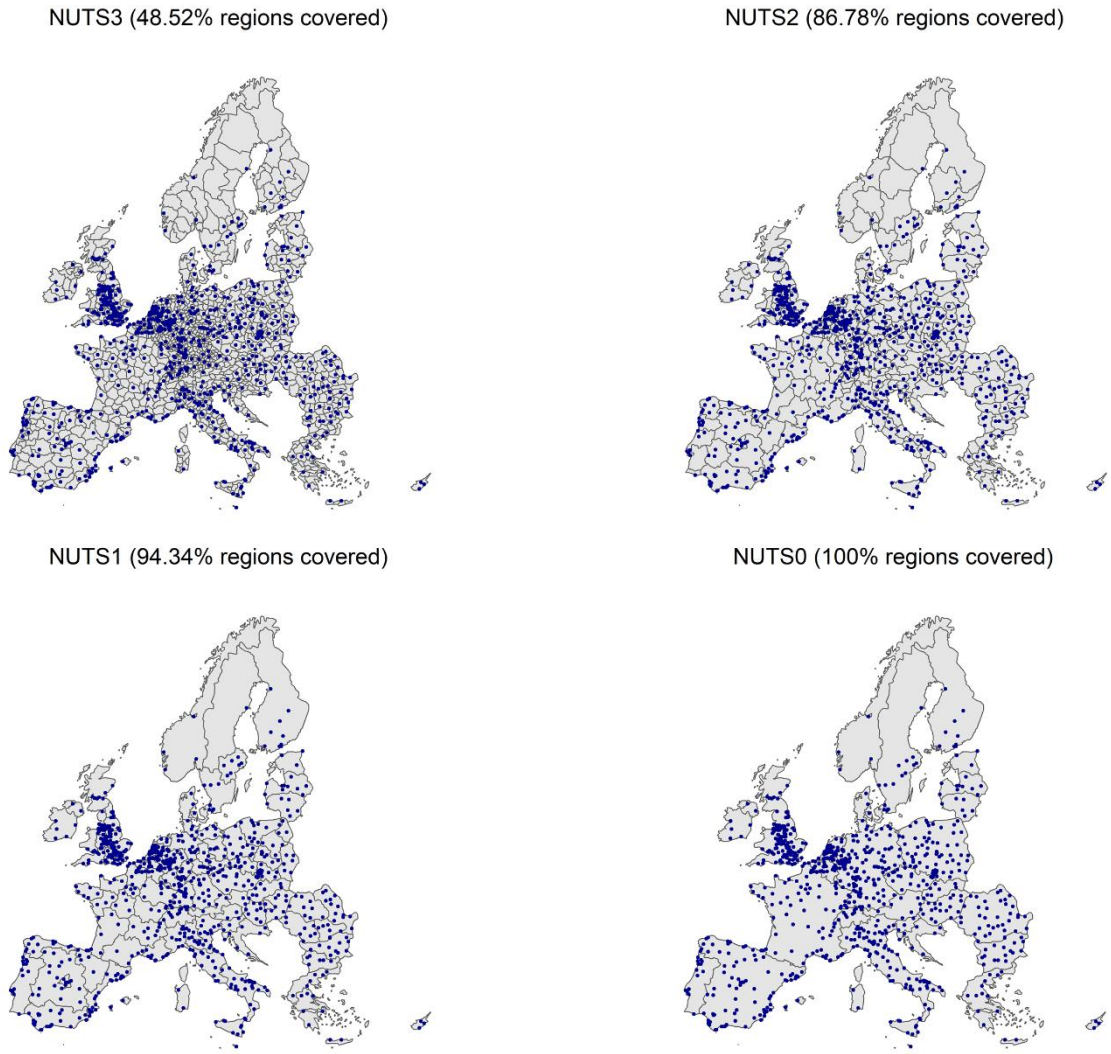

Figure S3: Our analysis is based on a time series epidemiological study of 854 European cities.[1] The maps depict the percentage of NUTS regions including at least one sampled city at various NUTS aggregation levels.

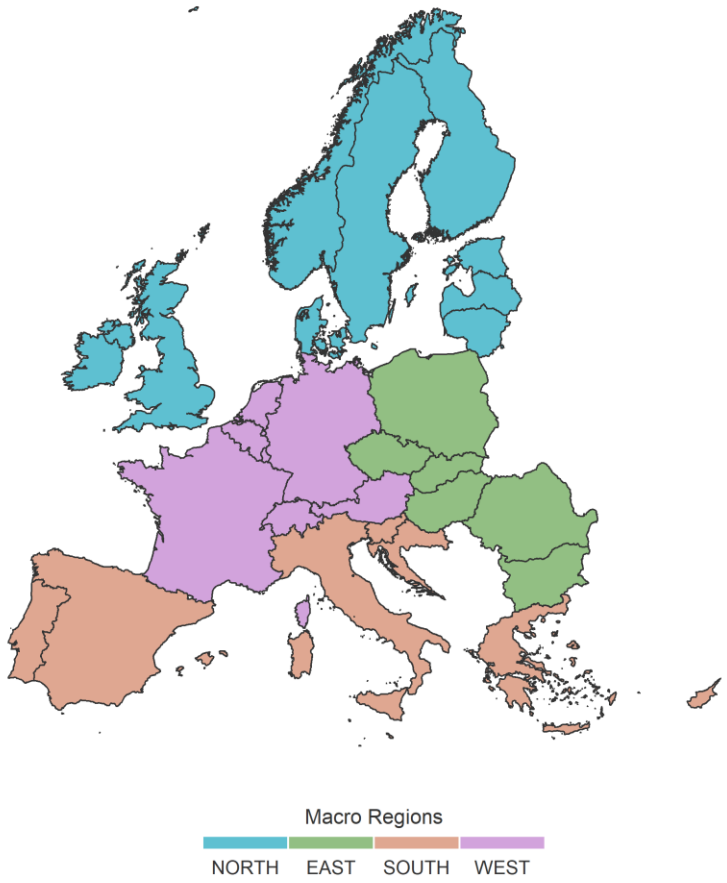

Figure S4: For the joint analysis of heat and cold mortality, and following the United Nation's M49 geoscheme[6], we divide Europe into four large macro areas or clusters based on shared socioeconomic and epidemiological characteristics, as depicted in Figure 1.

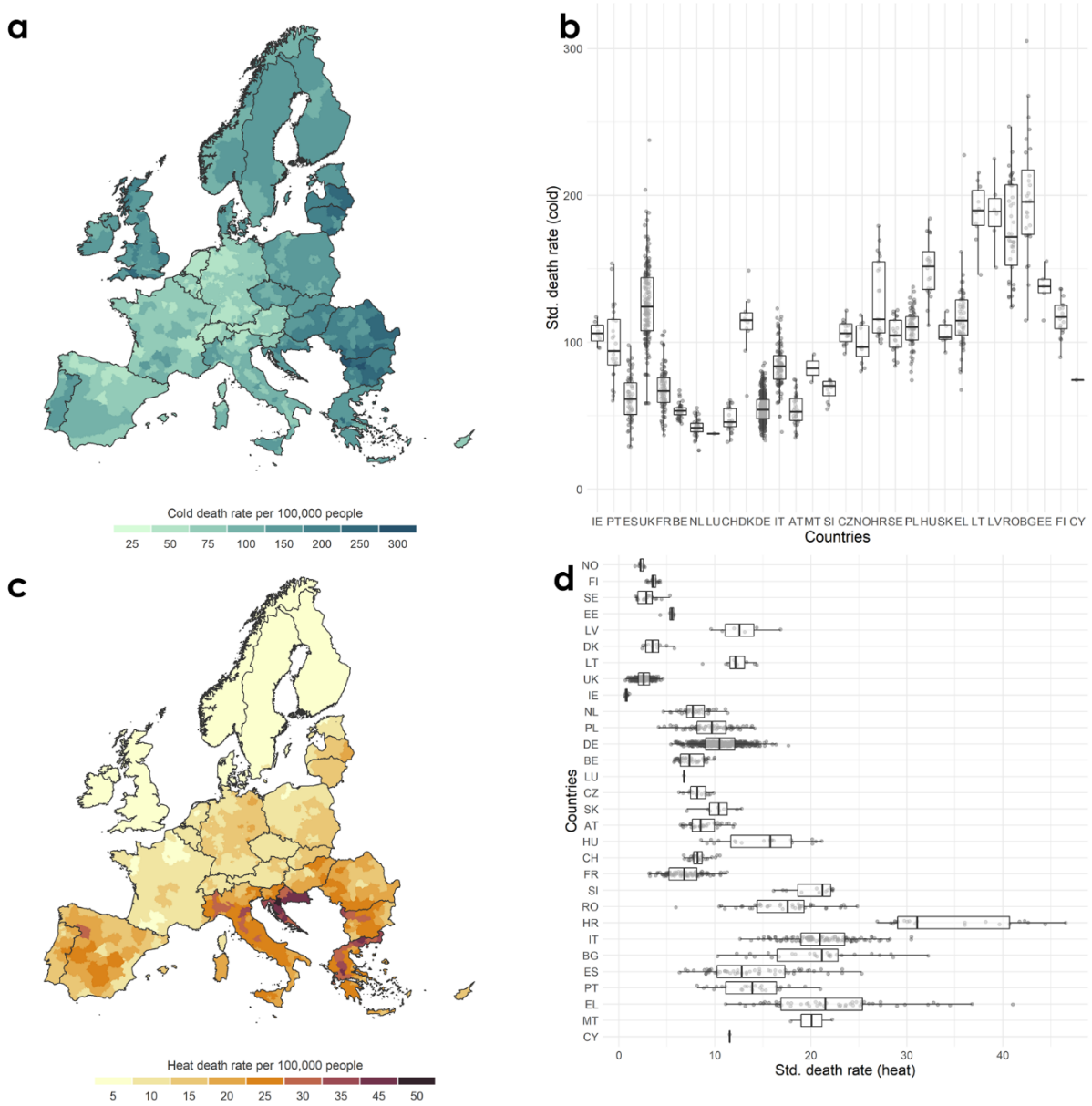

Figure S5: a,c Maps of standardised death rates per 100,000 people for cold-related (a) and heat-related (c) mortality based on 1991-2020 climatology and population data for the year 2020. **b,d** Standardised death rates for cold (b) and heat (d) ordered by country-centroid longitude and latitude, respectively. Each dot denotes a region. Boxes are centred at the median. The lower and upper hinges correspond to the first and third quartiles (the 25th and 75th percentiles). Whiskers extends from the hinge to ± 1·5*IQR. Overseas territories were excluded from the analysis.

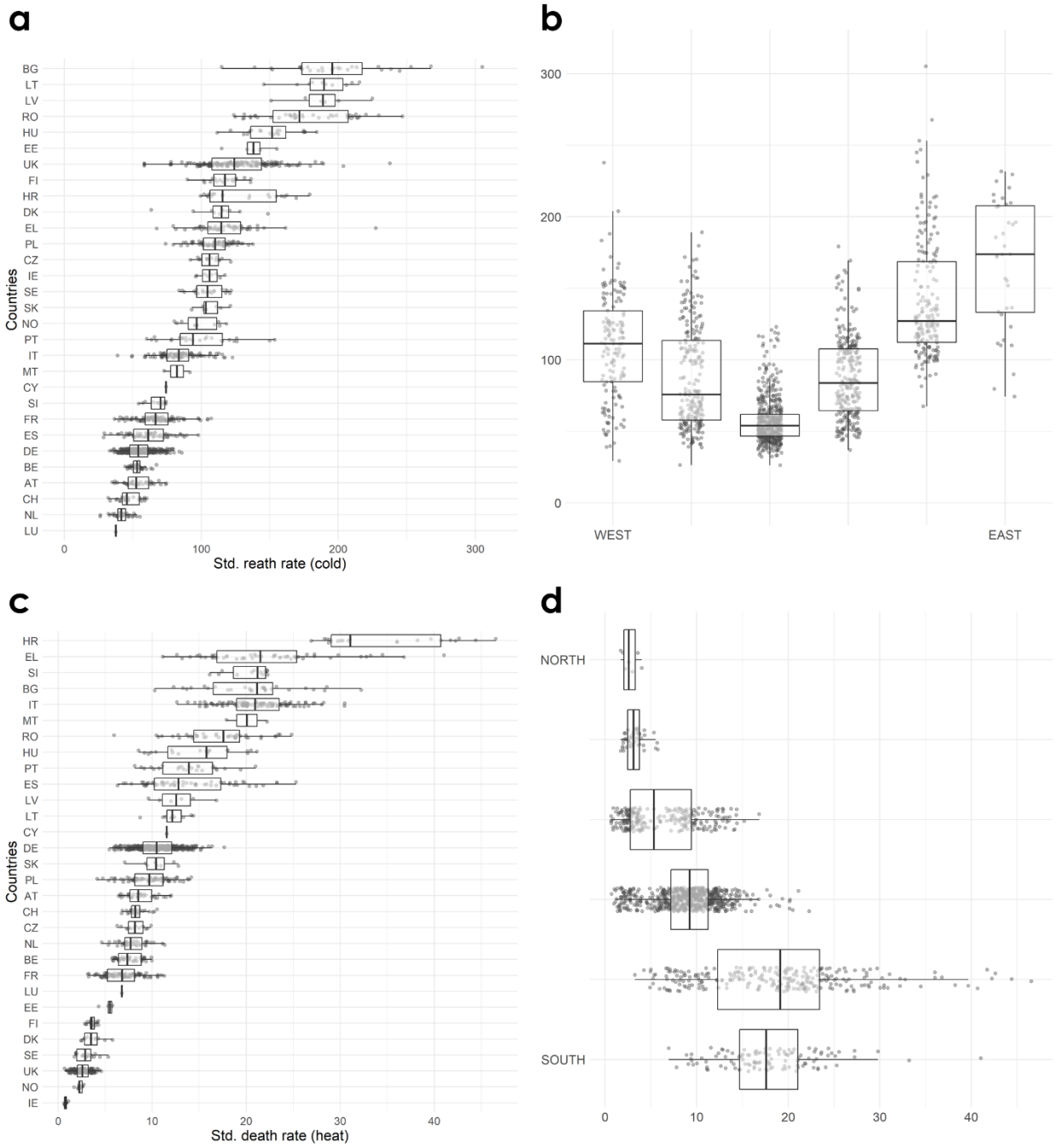

Figure S6: Average (1991–2020) standardised death rates in the 30 analysed countries. Panels **a** (cold) and **c** (heat) are ordered by country-median standardised death rates. Note the difference in scale between cold and heat death rates. **b,d** Standardised death rates grouped by longitude bins [b, cold, range (in decimal degrees): -9·18–33·22] and latitude bins [d, heat, range (in decimal degrees): 35·05–69·72], respectively.

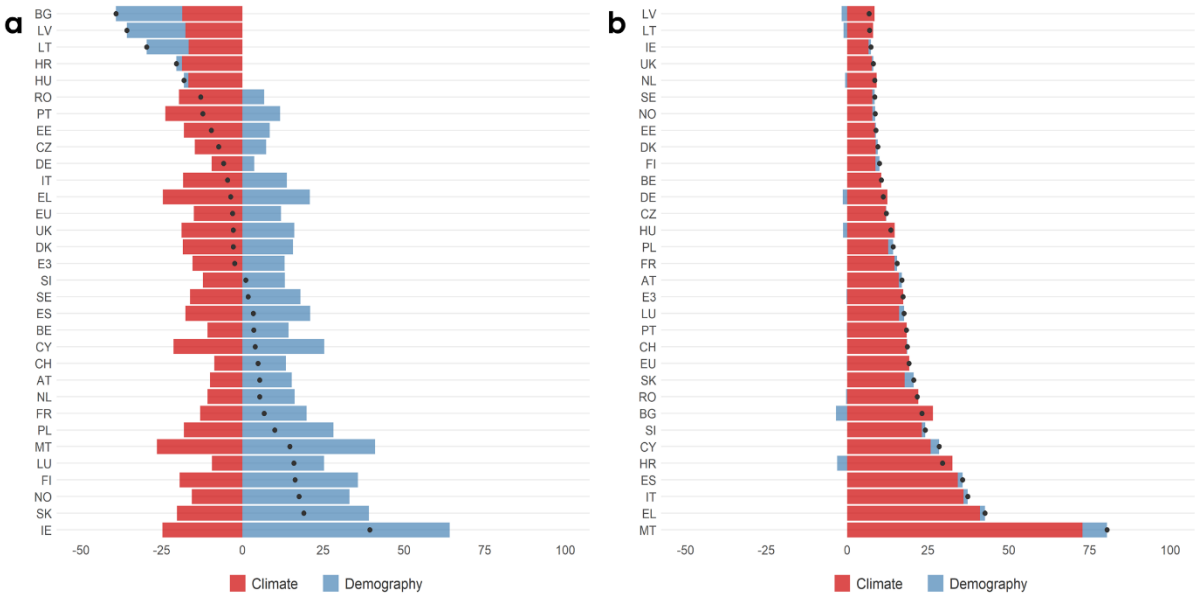

Figure S7: a,b Contribution of climate warming and demographic changes (lower fertility and declining death rates) to the variations projected in Fig.3 (a, cold) and (b, heat). Contributions were obtained as the difference between the time series simulations subject to demographic changes and under the absence of them. Black dots represent the total joint effect on the respective country death rates. Country codes are described in Table S2 (appendix p 5). Numeric values of the projected contributions are provided in Table S4 (appendix p 7).

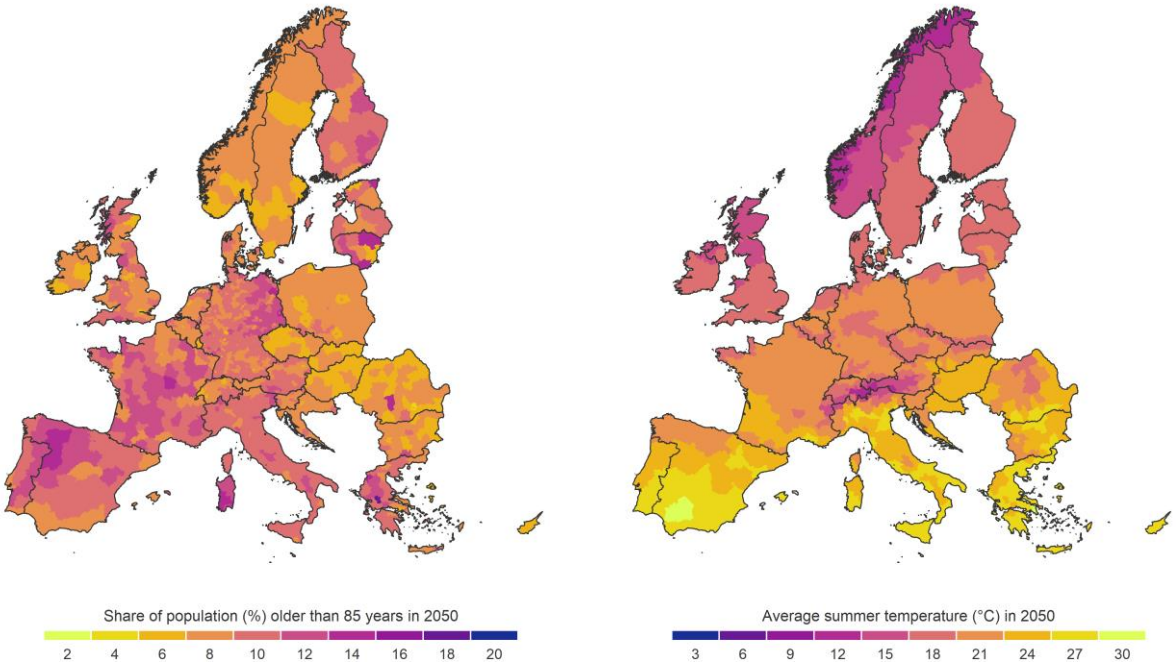

Figure S8: As depicted in Figure 4, heat death hotspots in year 2050 are determined by two separate components, which are plotted here individually: the regional share of the population older than 85 years (left) and the projected regional average summer temperature (right).

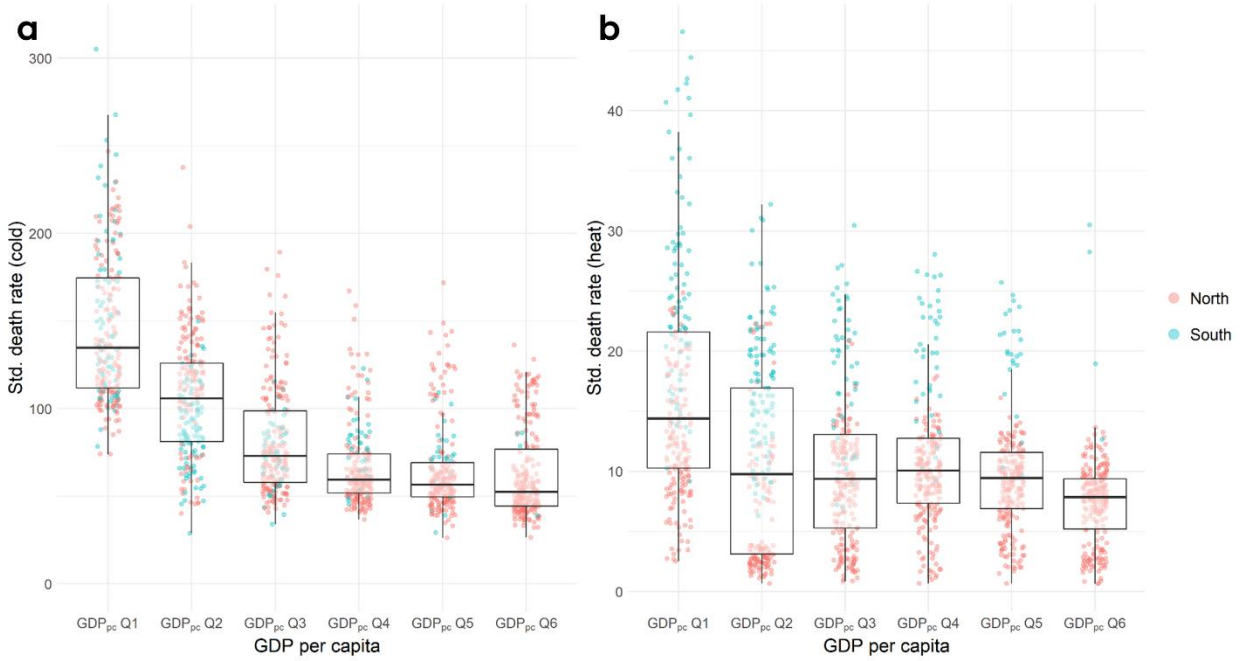

Figure S9: Average (1991–2020) standardised death rates for (**a**) cold-related and (**b**) heat-related mortality, ordered by GDP per capita quantiles and classified by Northern and Southern countries. Each quantile (bin) contains the same number of regions. We selected BG, CY, EL, ES, HR, IT, MT, and PT as 'South' countries. The remaining countries analysed were considered 'North' areas.

Supplementary References

1 Masselot P, Mistry M, Vanoli J, *et al.* Excess mortality attributed to heat and cold: a health impact assessment study in 854 cities in Europe. *The Lancet Planetary Health* 2023; **7**: e271–81.

2 Gasparrini A, Armstrong B, Kenward MG. Distributed lag non-linear models. *Statistics in Medicine* 2010; **29**: 2224–34.

3 Gasparrini A, Guo Y, Hashizume M, *et al.* Mortality risk attributable to high and low ambient temperature: a multicountry observational study. *The Lancet* 2015; **386**: 369–75.

4 Gasparrini A, Armstrong B. Reducing and meta-analysing estimates from distributed lag non-linear models. *BMC Med Res Methodol* 2013; **13**: 1.

5 Sera F, Armstrong B, Blangiardo M, Gasparrini A. An extended mixed-effects framework for meta-analysis. *Statistics in Medicine* 2019; **38**: 5429–44.

6 United Nations. Standard country or area codes for statistical use (M49). https://unstats.un.org/unsd/methodology/m49/ (accessed Dec 10, 2023).

7 Robinson GK. That BLUP is a Good Thing: The Estimation of Random Effects. *Statist Sci* 1991; **6**. DOI:10.1214/ss/1177011926.

8 Gasparrini A, Armstrong B, Kenward MG. Multivariate meta-analysis for non-linear and other multi-parameter associations. *Statistics in Medicine* 2012; **31**: 3821–39.

9 Armstrong BG, Gasparrini A, Tobias A, Sera F. Sample size issues in time series regressions of counts on environmental exposures. *BMC Med Res Methodol* 2020; **20**: 15.

10 IPCC. Climate Change 2021 – The Physical Science Basis: Working Group I Contribution to the Sixth Assessment Report of the Intergovernmental Panel on Climate Change, 1st edn. Cambridge University Press, 2023 DOI:10.1017/9781009157896.

11 Hsiang S, Kopp R, Jina A, *et al.* Estimating economic damage from climate change in the United States. *Science* 2017; **356**: 1362–9.

12 Maule CF, Mendlik T, Christensen OB. The effect of the pathway to a two degrees warmer world on the regional temperature change of Europe. *Climate Services* 2017; **7**: 3–11.

13 Mentaschi L, Alfieri L, Dottori F, *et al.* Independence of Future Changes of River Runoff in Europe from the Pathway to Global Warming. *Climate* 2020; **8**: 22.

14 Ballester J, Quijal-Zamorano M, Méndez Turrubiates RF, *et al.* Heat-related mortality in Europe during the summer of 2022. *Nat Med* 2023; published online July 10. DOI:10.1038/s41591-023-02419-z.

15 WMO. WMO update: 50:50 chance of global temperature temporarily reaching 1.5°C threshold in next five years. World Meteorological Organization. 2022; published online May 9. https://wmo.int/news/media-centre/wmo-update-5050-chance-of-global-temperature-temporarily-reaching-15degc-threshold-next-five-years (accessed March 13, 2024).

16 Hermanson L, Smith D, Seabrook M, *et al.* WMO Global Annual to Decadal Climate Update: A Prediction for 2021–25. *Bulletin of the American Meteorological Society* 2022; **103**: E1117–29.

17 Jenkins K, Kennedy-Asser A, Andrews O, Lo YTE. Updated projections of UK heat-related mortality using policy-relevant global warming levels and socio-economic scenarios. *Environ Res Lett* 2022; **17**: 114036.

18 Huber V, Krummenauer L, Peña-Ortiz C, *et al.* Temperature-related excess mortality in German cities at 2 °C and higher degrees of global warming. *Environmental Research* 2020; **186**: 109447.

19 Vicedo-Cabrera AM, De Schrijver E, Schumacher DL, Ragettli MS, Fischer EM, Seneviratne SI. The footprint of human-induced climate change on heat-related deaths in the summer of 2022 in Switzerland. *Environ Res Lett* 2023; **18**: 074037.

20 De Schrijver E, Sivaraj S, Raible CC, Franco OH, Chen K, Vicedo-Cabrera AM. Nationwide projections of heat- and cold-related mortality impacts under various climate change and population development scenarios in Switzerland. *Environ Res Lett* 2023; **18**: 094010.

21 García-León D, Casanueva A, Standardi G, Burgstall A, Flouris AD, Nybo L. Current and projected regional economic impacts of heatwaves in Europe. *Nat Commun* 2021; **12**: 5807.

22 Tobías A, Íñiguez C, Royé D. From Research to the Development of an Innovative Application for Monitoring Heat-Related Mortality in Spain. *Environ Health* 2023; : envhealth.3c00134.

23 Copernicus Climate Change Service (C3S). Europe in 2023: Europe's contrasting summer. European State of the Climate 2023. 2024. https://climate.copernicus.eu/esotc/2023/europes-contrasting-summer (accessed Dec 13, 2021).

24 Ballari D, Giraldo R, Campozano L, Samaniego E. Spatial functional data analysis for regionalizing precipitation seasonality and intensity in a sparsely monitored region: Unveiling the spatio-temporal dependencies of precipitation in Ecuador. *Intl Journal of Climatology* 2018; **38**: 3337–54.